Mobility edge in long-range interacting many-body localized systems

Rozhin Yousefjani^{1,*} and Abolfazl Bayat^{1,†}

¹Institute of Fundamental and Frontier Sciences, University of Electronic Science and Technology of China, Chengdu 610051, China

As disorder strength increases in disordered many-body systems a new structure of matter, the so-called many-body localized phase, emerges across the whole spectrum. This transition is energy dependent, a phenomenon known as mobility edge, such that the mid-spectrum eigenstates tend to localize at larger values of disorder in comparison to eigenstates near the edges of the spectrum. Many-body localization becomes more sophisticated in long-range interacting systems. Here, by focusing on several quantities, we draw the phase diagram as a function of disorder and energy spectrum, for a various range of interactions. We show that long-range interaction enhances the localization effect and shifts the phase boundary towards smaller values of disorder. In addition, we determine the relevant critical exponent, with which a diverging length scale emerges in the system, along the mobility edge. Our analysis establishes a hierarchy among the quantities that we have studied concerning their convergence speed towards their thermodynamic limit. Indeed, we show that deliberately decohering a subsystem can mitigate finite-size effects and provide results in line with the analytical predictions at the thermodynamic limit.

I. INTRODUCTION

Ergodicity principle, as the foundation of statistical physics, is violated in disordered systems. Many-Body Localization (MBL) is the primary example of such phenomenon in interacting disordered systems which has attracted lots of attention in recent years [1–5]. Several features of the MBL have been characterized through static and dynamical analyses, including: Poisson-like level statistics [6–9], area-law entangled eigenstates [10, 11], logarithmic entanglement growth [12– 18], suppression of transport [19–23], power-law decay of local correlations [24-29], and the emergence of memory [30-37]. Unlike quantum phase transition, which is a property of the ground state [38], the transition from ergodic to MBL takes place across the whole spectrum, as disorder strength increases. This makes the detection and characterization of the MBL transition very challenging [39-42]. In fact, each energy eigenstate localizes at a different disorder strength, a phenomenon that is called mobility edge which has been explored theoretically [9, 10, 43-51] and observed experimentally [52]. Since MBL is a property of the whole spectrum, its numerical investigation is mostly limited to exact diagonalization of small systems. This makes it very challenging to extract information about the thermodynamic limit. Thanks to the recent development of quantum simulators, MBL experiments have been implemented in various platforms such as superconducting devices [40, 42, 52-58], cold atoms in optical lattices [41, 59–64], ion traps [65–67], nitrogen-vacancy centers in diamond [68, 69], and photonic systems [70].

Perhaps the most challenging problem in the MBL context is the characterization of the MBL transition and its corresponding mobility edge [5, 71–74]. In a crucial analytical contribution by Harris [75], which has been extended by others [76, 77], the MBL transition has been described as a continuous second-order phase transition which is accompanied by the emergence of a diverging length scale ($\sim |W-W_c|^{-\nu}$)

*Electronic address: RozhinYousefjani@uestc.edu.cn †Electronic address: abolfazl.bayat@uestc.edu.cn in the system. Here, W is the strength of disorder, W_c is critical disorder strength beyond which the system is localized, and v is a critical exponent that satisfies $v \ge 2/d$ in a d-dimensional system (also known as Harris criteria). Surprisingly, most of the conventional quantities that have been studied in 1-dimensional MBL system, such as von Neumann entropy, violate Harris criteria and result in $\nu \sim 1$ [9, 31]. There are some exceptions, such as Schmidt gap [30, 78] and diagonal entropy [30, 79, 80], which either satisfy the Harris criteria or at least violate it less by giving $v\sim2$. There are two distinct explanations for the inconsistency of numerical simulations with the Harris bound: (i) the system sizes that are available to exact diagonalization are too small to capture convergence towards the thermodynamic limit [71, 73]; and (ii) describing the MBL transition as a second-order phase transition is not valid and one has to explain it as a Kosterlitz-Thouless type [81–89]. It is worth emphasizing that in most of the literature ν is only computed for the mid-spectrum eigenstates and its behavior across the spectrum is hardly explored. These hot debates show that characterization of the MBL transition and its corresponding mobility edge is far from being settled.

Investigation of the MBL beyond the conventional nearestneighbor interactions may open new questions. Long-range interactions, such as Coulomb, dipole-dipole and van der Waals, are of utmost importance as they naturally arise in many systems. On experimental side, some of the quantum simulators, such as ion-traps [65–67] and Rydberg atoms [41, 63, 64], are naturally governed by such interactions. The existence of an MBL phase [90-101] and its principal properties in long-range interacting systems is still hotly debated. For instance, while earlier studies of the MBL in long-range systems suggested an algebraic growth of entanglement entropy [101–108], recent work shows non-algebraic behavior through long-time numerical simulations [109]. Interestingly, different types of long-range couplings can have different effects on the system. While long-range tunneling can increase delocalization, long-range (Ising) interaction enhances localization [90, 101, 106, 109]. Several important issues are still open in long-range MBL systems, including: (i) the phase boundary, and thus the mobility edge, along the energy spectrum as the strength of long-range interaction varies; and (ii)

the value of ν and its consistency with Harris bound along the mobility edge.

In this paper, we aim to address these issues through considering several quantities, including level statistics ratio, entanglement entropy, diagonal entropy, and Schmidt gap. We draw the phase diagram for each of these quantities across the whole spectrum as the strength of long-range interaction varies. In fact, we show that long-range interaction enhances the localization and shifts the mobility edge towards smaller values of W_c . In addition, we determine ν along the mobility edge and show that its value can indeed be energy dependent. Our analysis establishes a hierarchy among our quantities with respect to the values that they give to W_c and ν . Interestingly, we show that for very wide range of long-range interactions, the diagonal entropy can give results fully consistent with the Harris criteria.

The paper is organized as follows. We begin by introducing the benchmark model in section II and the physical observables that we used to study the transition in section III. After providing a detailed discussion about the method that we used for extracting the critical values and critical exponents in section IV, we present the main results in section V of the paper. Our main results are briefly summarized in section VI.

II. MODEL.

We consider an open-boundary chain of N spin-1/2 particles in the presence of a random magnetic field. While spin tunneling is restricted between nearest-neighbor sites, interaction between particles is taken to be long-range which algebraically decays by exponent $\alpha>0$. The Hamiltonian reads

$$H = -\sum_{i=1}^{N-1} (S_i^x S_{i+1}^x + S_i^y S_{i+1}^y) - \sum_{i \neq j=1}^N \frac{1}{|i-j|^\alpha} S_i^z S_j^z + \sum_{i=1}^N h_i S_i^z, (1)$$

here $S_i^{(x,y,z)}$ are the spin-1/2 operators for qubit i, and h_i denotes a random magnetic field in the \hat{z} direction acting on qubit i which is drawn from a uniform distribution [-W, W], with W being the strength of disorder. Note that, by varying α we can smoothly interpolate between a fully connected graph (i.e. α =0) and standard nearest-neighbor 1-dimensional chain (i.e. $\alpha \rightarrow \infty$). In this paper, we investigate the transition of an ergodic phase into a many-body localized one, for different values of α , as the disorder strength W increases. In particular, the transition along the energy spectrum, known as mobility edge, will be studied through several different quantities. As the result we fully determine the phase diagram of the system as a function of two control parameters (W, α) .

III. METHODS AND QUANTITIES

To characterize the transition between the ergodic and the MBL phases, we consider four observables including averaged gap ratio, half-chain entanglement entropy, half-chain

diagonal entropy, and half-chain Schmidt gap. Before providing exact definitions of these four quantities, we would like to explain our numerical approach. For systems of length $N=10, 11, \dots, 15$, we provide 2000 (for $N \le 13$) to 1000 (for N=14,15) sample realizations of the random field. We restrict ourselves to the subspace of S_{tot}^z =0 or S_{tot}^z =1/2 (with $S_{tot}^z = \sum_i S_i^z$ for even and odd N's, respectively. For each set of random fields and with the means of exact diagonalization, we generate M eigenstates $\{|E_k\rangle\}$ of the Hamiltonian H around the rescaled energy $\varepsilon \in \{0.2, \cdots, 0.8\}$, where ε 's have been calculated as $\varepsilon = (E_{max} - E)/(E_{max} - E_{min})$ in which E_{max} and E_{min} are the extremal eigenvalues of H. For every eigenstate $|E_k\rangle$ one can compute one of the aforementioned quantities which results in the value O_k . To have an average behavior of eigenstates at energy ε , one can average over the M=50 obtained eigenstates around that energy which results in $\langle O \rangle = 1/M \sum_{k=1}^{M} O_k$. In addition, in order to have a meaningful quantity to investigate MBL, one has to also average over different random samples which is denoted by $\langle O \rangle$. These averaged quantities are used for establishing finite-size scaling analyzes and characterizing the critical properties of the transition.

Our first quantity is the gap ratio r which is a well-established tool to study statistical properties of the energy levels $\{E_k\}$ of the Hamiltonian H. For energy gaps $\delta_k = E_{k+1} - E_k$, the ratio $r_k = \min(\delta_{k+1}, \delta_k) / \max(\delta_{k+1}, \delta_k)$ and its average $\langle r \rangle$, over energy levels and sample realizations, can diagnose a global change in the spectral statistics. While in the MBL phase the energy levels are spaced according to Poisson statistics, yielding $\langle r \rangle = 2 \ln 2 - 1 \approx 0.386$, in the ergodic phase the strong repulsion between neighboring levels causes statistics that match with those of the Gaussian orthogonal ensembles, resulting in $\langle r \rangle \approx 0.5307$.

The second quantity of interest is the entanglement entropy S_{FF} , which is a widely used tool for quantifying entanglement between two complementary parts of a pure manybody system. For any given eigenstate $|E_k\rangle$ one can obtain the reduced density matrix $\rho_{r}^{(k)}$ by tracing out $\lceil L/2 \rceil$ qubits on the right side of the chain. Therefore, the entanglement entropy between left and right cuts of the chain is defined as $S_{EE}(\rho_I^{(k)}) = -\text{Tr}[\rho_I^{(k)} \ln \rho_I^{(k)}]$. In the ergodic phase, the eigenstates are expected to behave like a random pure state and exhibit a volume law entanglement entropy determined by Page entropy $S_{EE}^{P} = (1 - \mathcal{D}_{L})/2\mathcal{D}_{R} + \sum_{k=\mathcal{D}_{R}+1}^{\mathcal{D}_{L}} 1/k$ with \mathcal{D}_{L} and \mathcal{D}_{R} as the Hilbert space dimensions of the left and right chain cuts [110]. In contrast, in the localized phase due to the emergent integrability the eigenstates exhibit an area-law entanglement. Therefore, in deep ergodic and MBL phases, one expects to have $\overline{\langle S_{EE} \rangle}/S_{EE}^P \sim 1$ and $\overline{\langle S_{EE} \rangle}/S_{EE}^P \sim 0$, respectively, for the averaged entanglement entropy.

As the third quantity, we consider the diagonal entropy of a subsystem. Replacing $\rho_L^{(k)}$ in $S_{EE}(\rho_L^{(k)})$ by the decohered density matrix $\varrho_L^{(k)}$, in which all the off-diagonal elements in computational basis are set to zero, results in the diagonal entropy $S_{DE}(\varrho_L^{(k)}) = -\text{Tr}[\varrho_L^{(k)} \ln \varrho_L^{(k)}]$. This quantity has recently been used in the context of MBL [30, 79, 80]. In the ergodic phase, the diagonal entropy provides an upper bound for en-

tanglement entropy, namely $S_{DE}(\varrho_L^{(k)}) \geqslant S_{EE}(\rho_L^{(k)})$. However, in the deep localized phase there main close to each other, namely $S_{DE}(\varrho_L^{(k)}) \sim S_{EE}(\rho^{(k)})$, as $\rho_L^{(k)}$ and its decohered state $\varrho_L^{(k)}$ have high fidelity. Analogues to the entanglement entropy, by calculating the maximum diagonal entropy for a typical random pure state as $S_{DE}^P \simeq \ln(0.48\mathcal{D}_L) + \ln(2)$ [111, 112], one can determine two limiting behaviors $\overline{\langle S_{DE} \rangle}/S_{DE}^P \sim 1$ and $\overline{\langle S_{DE} \rangle}/S_{DE}^P \sim 0$ for the ergodic and localized phases, respectively.

The fourth and our final indicator is the Schmidt gap of the reduced density matrix $\rho_L^{(k)}$ which can be calculated by using its two largest eigenvalues, denoted by $\lambda_1^{(k)}$ and $\lambda_2^{(k)}$, as $\Delta(\rho_L^{(k)}) = \lambda_1^{(k)} - \lambda_2^{(k)}$. In contrast to the entanglement entropy which consider all the spectrum of $\rho_L^{(k)}$, the Schmidt gap only focuses on two dominant eigenvalues. In the ergodic phase $\rho_L^{(k)}$ is expected to be a thermal state with infinite temperature (at least for mid-spectrum eigenstates) which results in $\overline{\langle \Delta \rangle} \sim 0$. In the localized phase the reduced density matrix $\rho_L^{(k)}$ tends to become a pure state and thus the Schmidt gap increases such that in the deep localized phase, one has $\overline{\langle \Delta \rangle} \rightarrow 1$.

IV. FINITE-SIZE SCALING

Finite-size scaling analysis is a standard technique for extracting the thermodynamic properties of a many-body system around its critical point using finite size systems. We use this method to: (i) characterize the behavior of various quantities around the transition point at different energy scales along the mobility edge; (ii) draw a precise phase diagram in the (W, ε) plane for various choices of α ; and (iii) extract the relevant critical exponent ν as a function of energy ε for different values of α . In this paper, we treat the ergodic-MBL transition as a second-order phase transition. Therefore, for the quantities of interest, we suggest an ansatz of the form

$$\overline{\langle O \rangle} = f((W - W_c)N^{1/\nu}),$$
 (2)

where N is the system size, W_c is the transition point, ν is the exponent that describes the emergence of a diverging length scale ($\sim |W - W_c|^{-\nu}$) near the transition point and $f(\cdot)$ is an arbitrary scaling function which is specific for any quantity $\langle \overline{O} \rangle$. This choice of ansatz can be used in two different ways: (i) intersection analysis which is based on the fact that at $W = W_c$ the dependence on N disappears for all quantities $\langle O \rangle$; and (ii) finite-size scaling analysis in which the plots of $\overline{\langle O \rangle}$ as a function of $(W - W_c)N^{1/\nu}$ for different choices of N collapse on each other. While the first approach (i.e. intersection method) helps to estimate W_c simply, the second one (i.e. finite-size scaling analysis) allows to precisely determine the values of both W_c and ν through a more elaborate optimization scheme. The latter can be achieved through optimization of W_c and ν for obtaining the best data collapse of curves for different system sizes. To perform such optimization, one can define a quality parameter Q, as a cost function of the process, which has to be minimized for obtaining the best data collapse of different curves [113, 114]. One of such quality parameters is defined and discussed in the Appendix. A perfect data collapse results in Q=1 and any deviation from such a perfect data collapse makes Q larger.

The ansatz in Eq. (2) is used for three different quantities, namely the normalized entanglement entropy $\overline{\langle S_{\scriptscriptstyle EE}\rangle}/S_{\scriptscriptstyle EE}^{P}$, the normalized diagonal entropy $\overline{\langle S_{\scriptscriptstyle DE}\rangle}/S_{\scriptscriptstyle DE}^{P}$, and the Schmidt gap $\overline{\langle \Delta\rangle}$, at different energy scale ε and long-range interaction strength α . For any given choice of ε and α the intersection approach or finite-size scaling analysis can be employed to estimate W_c and possibly ν (which is only doable through finite-size scaling). However, the values extracted from different quantities may slightly differ due to our finite system sizes and various convergence speeds of such quantities.

In this section, we focus on the mid spectrum, namely ε =0.5, and a fairly long-range interacting system with α =0.5. We consider both intersection and finite-size scaling analyses. In the next section, we extend our analysis to the whole energy spectrum and a wide range of α . In Fig. 1(a), we plot the normalized entanglement entropy $\overline{\langle S_{\it EE} \rangle}/S_{\it EE}^{\it P}$ as a function of disorder strength $\it W$ for different system sizes. By increasing W, the entanglement entropy deviates from its value for a random pure state, namely S_{EE}^{P} , and tends to zero. As predicted by our ansatz, at $W = W_c$ the length becomes irrelevant and the curves for different length should intersect, signaling the onset of the transition between the ergodic and MBL phases. This can be clearly seen in Fig. 1(a) in which curves for different system sizes intersect at a narrow region. The small fluctuations at the intersection of different curves are a finite-size effect which makes it difficult to extract a precise estimation of W_c . Therefore, one has to exploit finite-size scaling analysis as a more precise approach for characterizing the phase transition properties. In the inset of Fig. 1(a), we plot the normalized entanglement entropy $\overline{\langle S_{\scriptscriptstyle EE} \rangle}/S_{\scriptscriptstyle EE}^{\,P}$ as a function of $(W - W_c)N^{1/\nu}$ for different system sizes and collapse them through tuning W_c and ν . We use Python package pyfssa [115, 116] for finding the best curves collapse which results in $W_c^{EE} = 1.996 \pm 0.017$ and $v^{EE} = 0.971 \pm 0.026$ with quality $Q^{EE} = 8.744$.

The same intersection and finite-size scaling analyses can be repeated for other quantities. In Fig. 1(b), the normalized diagonal entropy $\overline{\langle S_{\scriptscriptstyle DE}\rangle}/S_{\scriptscriptstyle DE}^{P}$ is plotted as a function of W for various system sizes. The intersection of different curves signals the transition from ergodic to MBL. However, similar to the previous case, the fluctuation of the intersection point for different curves does not allow for a precise estimation of W_c . In the inset of this panel, we plot the normalized diagonal entropy as a function of $(W-W_c)N^{1/\nu}$ and tune W_c and ν for the best quality data collapse. This results in $W_c^{DE}=2.930\pm0.015$, and $\nu^{DE}=2.183\pm0.082$. The quality of the data collapse for these critical values is $Q^{DE}=2.145$. An immediate observation is that while W_c^{DE} is slightly larger than W_c^{EE} , the critical exponent ν^{DE} is much larger than ν^{EE} and is fully consistent with the Harris bound.

Finally, in Fig. 1(c) and its inset, we repeat the above analyses for the Schmidt gap $\overline{\langle \Delta \rangle}$. Unlike the previous two quantities, the Schmidt gap takes zero value in the ergodic phase and rises towards 1 in the MBL phase. The intersection of

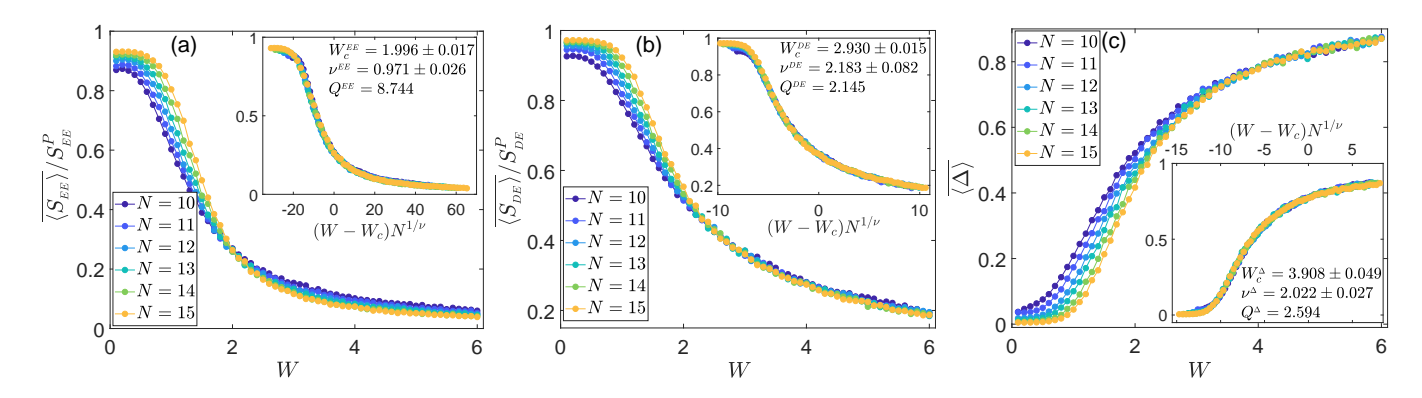


FIG. 1: (a) the normalized entanglement entropy $\overline{\langle S_{EE} \rangle}/S_{EE}^P$, (b) the normalized diagonal entropy $\overline{\langle S_{DE} \rangle}/S_{DE}^P$, and (c) the Schmidt gap $\overline{\langle \Delta \rangle}$ as a function of disorder strength W for different system sizes. All the quantities are obtained for long-range system with interaction's exponent α =0.5 in the mid spectrum ε =0.5. The insets represent the finite-size scaling analysis for extracting the critical combination (W_c , v). The quality of the data collapses have been determined by Q.

the curves in Fig. 1(c) takes place at a larger disorder strength than the two previous quantities. The finite-size scaling analysis in the inset of Fig. 1(c) results in W_c^{Δ} =3.908 ± 0.049 and v^{Δ} =2.022 ± 0.027, with the quality being Q^{Δ} = 2.594. Interestingly, the critical exponent v^{Δ} , extracted from the Schmidt gap, is also consistent with the Harris bound. This suggests that quantities such as the diagonal entropy and the Schmidt gap might be more suitable for emulating thermodynamic behavior using small system sizes. This is perhaps due to the faster convergence of these quantities in comparison with the von Neumann entropy.

V. PHASE DIAGRAM

As shown in the previous section, intersection analysis cannot precisely determine W_c and is also unable to extract the critical exponent ν . Therefore, in this section, we focus only on finite-size scaling analysis and extend it for all energy spectrum ε and various values of α .

For any given α and energy scale ε , performing finite-size scaling analysis extracts both the transition point W_c , and thus the mobility edge, and the critical exponent ν . In Figs. 2(a)-(f) we plot the averaged gap ratio $\langle r \rangle$ as a function of the energy ε and the disorder strength W for various values of α . By increasing the value of disorder strength, one can continuously move from the ergodic phase (light region) to the localized phase (dark region). The red, magenta, and yellow markers in these plots denote the transition points W_c^{EE} , W_c^{DE} , and W_c^{Δ} , respectively, obtained from finite-size scaling analysis for the normalized entanglement entropy $\overline{\langle S_{\it EE} \rangle}/S_{\it EE}^{\it P}$, the normalized diagonal entropy $\overline{\langle S_{\it DE} \rangle}/S_{\it DE}^{\it P}$, and the Schmidt gap $\overline{\langle \Delta \rangle}$, respectively. Three main features can be observed: (i) all considered quantities reveal a generic D-shape structure signifying energy dependent transition, i.e. the well-known many-body mobility edge; (ii) decreasing α (i.e. making the interaction more long-range) enhances the localization power such that the localization occurs for smaller values of W; and (iii) there is a hierarchical relationship among the considered quantities

such that their corresponding transition points follow

$$W_c^{\Delta} \ge W_c^{DE} \ge W_c^{EE} \tag{3}$$

While the first feature, mentioned above, is expected and has already been observed for MBL systems both analytically [9, 10, 43–51] and experimentally [52], the second feature is a special property of long-range interactions. Indeed, every spin configuration of the chain induces an effective Zeeman energy on a given site. Thus, the superposition of spin configurations can play like an effective random field and thus enhances the localization power. This is in full agreement with a recent analysis of Floquet MBL in long-range interacting systems [109]. The third feature is also an interesting observation that can have an important interpretation. While entanglement entropy accounts for the entanglement between the two parts of the system, the diagonal entropy and the Schmidt gap discard some information by ignoring the off diagonal terms of the reduced density matrix or ignoring its smaller eigenvalues. In fact, ignoring such partial information shifts the transition point W_c to higher values. In particular, for $\alpha \to \infty$, the transition point W_c found by the diagonal entropy and the Schmidt gap is closer to the values found by other quantities in larger system sizes [9, 30, 48, 73, 117]. This suggests that the diagonal entropy and Schmidt gap converge faster to their thermodynamic limit in comparison with von Neumann entropy and hence are more suitable for emulating the behavior of system at large scales.

As discussed in the previous section, apart from W_c our finite-size scaling analysis also provides the value of ν along the energy spectrum. In Fig. 3(a)-(f) we plot the critical exponent ν , obtained from finite-size scaling of different quantities, as a function of energy ε for various values of α . One can observe that for all values of α and ε there is a hierarchy for critical exponent ν obtained from different quantities, namely

$$\nu^{DE} \ge \nu^{\Delta} \ge \nu^{EE}. \tag{4}$$

Consistent with previous studies, the critical exponent obtained from the entanglement entropy, namely v^{EE} (depicted by red markers in Fig. 3) is always $v^{EE} \sim 1$ at all energy scales ε

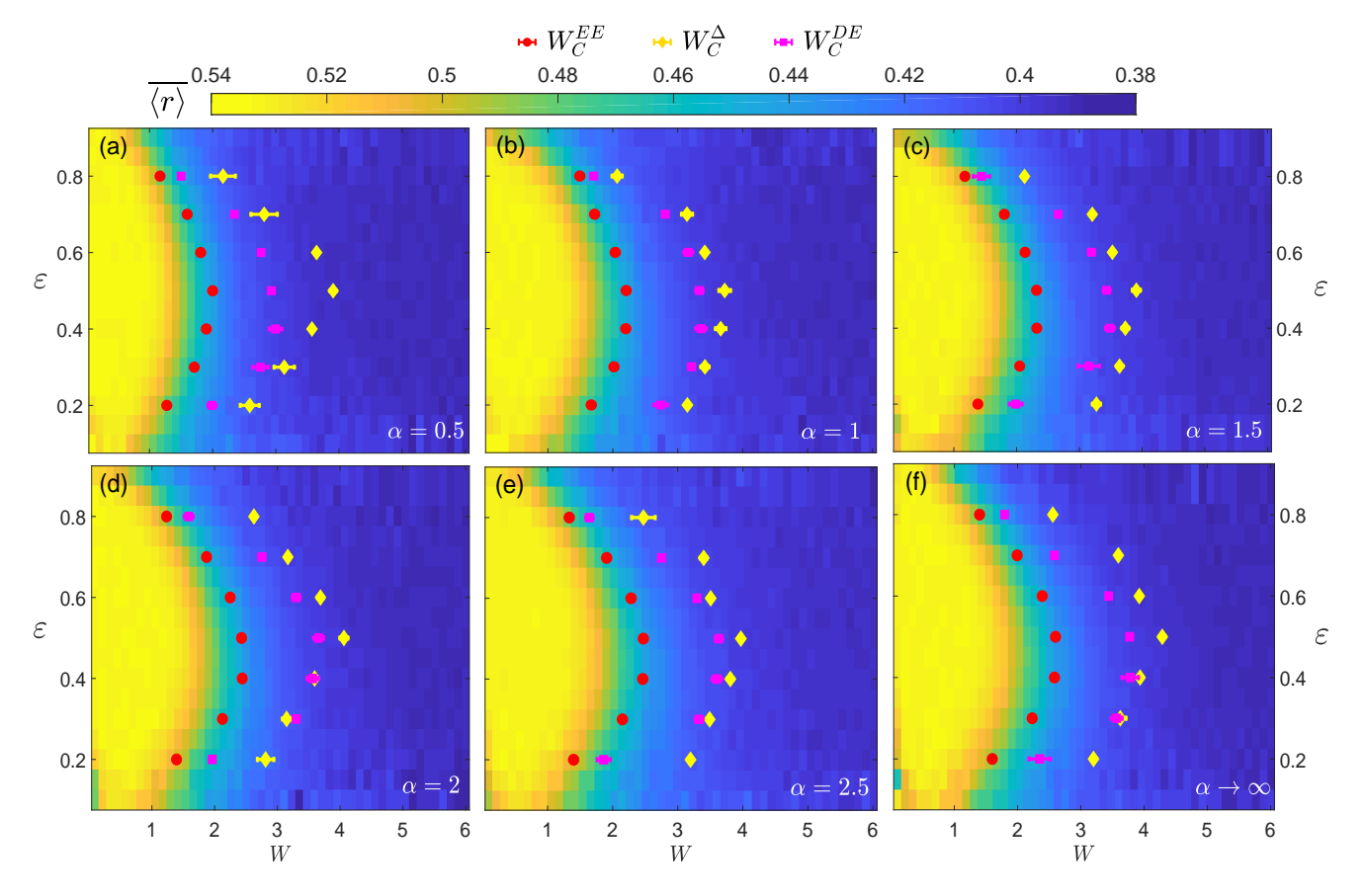


FIG. 2: The averaged gap ratio as function of energy ε and disorder strength W for different interaction ranges from (a) α =0.5 to (f) $\alpha \to \infty$. The red, magenta, and yellow markers in the panels denote the transition points W_c 's obtained from finite-size scaling analysis for the normalized entanglement entropy $\overline{\langle S_{EE} \rangle}/S_{EE}^P$, the normalized diagonal entropy $\overline{\langle S_{DE} \rangle}/S_{DE}^P$, and the Schmidt gap $\overline{\langle \Delta \rangle}$, respectively. In most of the data, the error bar which shows the standard error of the mean value is smaller than the size of the marker.

and for any given α . This, clearly, violates the Harris criteria which implies $v \ge 2$. Interestingly, the critical exponent obtained from the Schmidt gap, namely v^{Δ} (depicted by yellow markers in Fig. 3), shows more fluctuations along the energy spectrum and consistently gives higher values. In fact, for almost all values of α one estimates $1 < \nu^{\triangle} \le 2.5$, which is either perfectly matching with Harris bound or at least violates it with smaller degrees. The most interesting result is provided by the diagonal entropy. The critical exponent extracted from this quantity, namely v^{DE} (depicted by magenta markers in Fig. 3), is susceptible to both ε and α . For $0.5 \le \alpha \le 2$, regardless of the energy spectrum, one can find $2 \le v^{DE} \le 3$. This interval smoothly changes to $1.5 \le v^{DE} \le 3$ by decreasing the range of the interaction (i.e. increasing α) and for most of the data in the middle spectrum, one obtains $v^{DE} \simeq 2$. Based on the consistency with Harris prediction of $v \ge 2$, the diagonal entropy prevails over the other two quantities. In addition, the Schmidt gap seems to give more consistent results than the von Neuman entropy.

The fact that the diagonal entropy is more consistent with the analytic prediction of Harris bound, even in small systems, can be explained as faster convergence of this quantity towards the thermodynamic limit. In other words, while the diagonal entropy has already approached its thermodynamic

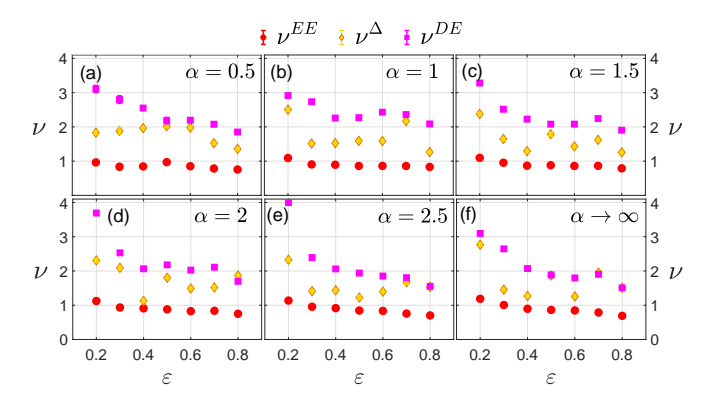


FIG. 3: The critical exponent ν 's as a function of energy scale ε for various interaction ranges from (a) α =0.5 to (f) α \rightarrow ∞ . These exponents are obtained from finite-size scaling analysis for different observables including the normalized entanglement entropy $\overline{\langle S_{\scriptscriptstyle DE} \rangle}/S_{\scriptscriptstyle EE}^{P}$ (red markers), the normalized diagonal entropy $\overline{\langle S_{\scriptscriptstyle DE} \rangle}/S_{\scriptscriptstyle DE}^{P}$ (magenta markers), and the Schmidt gap $\overline{\langle \Delta \rangle}$ (yellow markers).

limit with system sizes of N=15, the Schmidt gap and the entanglement entropy still show significant length dependence. Between the Schmidt gap and the entanglement entropy, the

former outperforms the other with respect to the speed of convergence and thus results in higher values of ν and less violation of Harris bound. Note that, for the computation of the diagonal entropy one has to artificially set the off-diagonal terms of the reduced density matrix to zero (in computational basis). This suggests that this artificial action emulates the behavior of the system in the thermodynamic limit. In fact, in the deep ergodic and MBL phases, the reduced density matrix is expected to be decohered in the thermodynamic limit due to being either maximally mixed (i.e. maximally entangled with the rest of the system) or a product pure state (i.e. fully separable), respectively. Interestingly, our observation shows that the decohering action can also better emulate the behavior of the system around the transition point in which coherence cannot be exactly zero. These results are consistent with previous studies of memory in MBL systems [31]. Measuring the diagonal entropy has also a practical advantage as one has to only measure the diagonal elements of the reduced density matrix and thus full state tomography, which is required for both the Schmidt gap and the von Neumann entropy, is not needed.

VI. CONCLUSION

In this paper, we have determined the phase boundary between ergodic and MBL phases along the energy spectrum, i.e. the mobility edge, for a Heisenberg spin-chain with longrange interaction in the presence of disordered magnetic field. This has been done using several quantities, including the level statistics ratio, the entanglement entropy, the diagonal entropy, and the Schmidt gap. We showed that long-range interaction enhances the localization effect and shifts the mobility edge in favor of MBL. By obtaining the critical properties of the MBL transition, i.e. W_c and ν , we established a hierarchy among considered quantities concerning the values that they give for W_c and ν . We show that discarding some information of the system, such as deliberately decohering the reduced density state of the half-chain in the diagonal entropy or ignoring its small eigenvalues in the Schmidt gap, help to achieve transition points which are closer to the values found in larger system analysis. Moreover, we observe that erasing the information related to coherence, can give critical exponents fully consistent with Harris criteria for a wide range of long-range interactions. This suggests that the diagonal entropy has a higher convergence speed and thus is more suited for capturing the large size behavior of the system.

VII. ACKNOWLEDGMENT

The authors acknowledge support from the National Key R&D Program of China (Grant No. 2018YFA0306703), the National Science Foundation of China (Grants No. 12050410253 and No. 92065115), and the Ministry of Science and Technology of China (Grant No. QNJ2021167001L).

Appendix

In the main text, we discussed that to precisely determine the transition point W_c and the critical exponent ν , we perform finite-size scaling analysis through plotting the rescaled data versus $(W-W_c)N^{1/\nu}$ and improve the quality of data collapse by tuning the parameters W_c and ν . To evaluate the quality of data collapse we followed the approach of Houdayer and Hartmann [113]. Assuming that i indexes the system size N_i and j indexes the disorder magnitude W_j with $W_1 < W_2 < \cdots < W_k$. For rescaled measured data $\{y_{ij}\}$ (e.g. the normalized entanglement entropy $\overline{\langle S_{EE} \rangle}/S_{EE}^P$ in different sizes and disorders) and its standard error $\{dy_{ij}\}$ at $x_{ij} = (W_j - W_c)N_i^{1/\nu}$, and also $\{\hat{y}_{ij}\}$ and $\{d\hat{y}_{ij}\}$ as the estimated values of the master curve and its standard error again at $x_{ij} = (W_j - W_c)N_i^{1/\nu}$, the quality function has been defined as [113]

$$Q = \frac{1}{N} \sum_{ij} \frac{(y_{ij} - \hat{y}_{ij})^2}{dy_{ij}^2 - d\hat{y}_{ij}^2}.$$
 (A1)

The sum in this function, which quantify the mean square of the weighted deviations from the master curve, only involves terms for which the estimated value \hat{y}_{ij} of the master curve at x_{ij} is defined. The number of such terms is \mathcal{N} . Clearly, Eq. (A1) provides objective identification of the combinations of (W_c, ν) resulting in statistically reasonable collapse. In our case, the reported critical values (W_c, ν) have been obtained by averaging all the combinations that yield to $Q \in [1, 1.2] Q_{min}$. To decrease the adverse effect of finite-size which can be too strong at the edges of the energy spectrum ε , we select the smallest values of N such that increasing N can not significantly affect the optimal combinations (W_c, ν) .

^[1] E. Altman, Nat. Phys. 14, 979 (2018).

^[2] D. A. Abanin and Z. Papić, Ann. Phys. **529**, 1700169 (2017).

^[3] D. A. Abanin, E. Altman, I. Bloch, and M. Serbyn, Rev. Mod. Phys. 91 (2019).

^[4] E. Altman and R. Vosk, Annu. Rev. Condens. Matter Phys. 6, 383 (2015).

^[5] D. A. Abanin, J. H. Bardarson, G. De Tomasi, S. Gopalakrishnan, V. Khemani, S. A. Parameswaran, F. Pollmann, A. C. Potter, M. Serbyn, and R. Vasseur, Ann. Phys. 427, 168415 (2021).

^[6] V. Oganesyan and D. A. Huse, Phys. Rev. B 75, 155111 (2007).

^[7] A. Pal and D. A. Huse, Phys. Rev. B 82, 174411 (2010).

^[8] V. Khemani, S. P. Lim, D. N. Sheng, and D. A. Huse, Phys. Rev. X 7, 021013 (2017).

^[9] D. J. Luitz, N. Laflorencie, and F. Alet, Phys. Rev. B 91, 081103 (2015).

^[10] J. A. Kjäll, J. H. Bardarson, and F. Pollmann, Phys. Rev. Lett. 113, 107204 (2014).

^[11] B. Bauer and C. Nayak, J. Stat. Mech.: Theory Exp 2013,

- P09005 (2013).
- [12] N. Laflorencie, arXiv:2112.09102.
- [13] J. H. Bardarson, F. Pollmann, and J. E. Moore, Phys. Rev. Lett. 109, 017202 (2012).
- [14] G. D. Chiara, S. Montangero, P. Calabrese, and R. Fazio, J. Stat. Mech. 2006, P03001 (2006).
- [15] M. Žnidarič, T. c. v. Prosen, and P. Prelovšek, Phys. Rev. B 77, 064426 (2008).
- [16] M. Serbyn, Z. Papić, and D. A. Abanin, Phys. Rev. Lett. 110, 260601 (2013).
- [17] R. Vosk and E. Altman, Phys. Rev. Lett. 110, 067204 (2013).
- [18] F. Andraschko, T. Enss, and J. Sirker, Phys. Rev. Lett. 113, 217201 (2014).
- [19] K. Agarwal, S. Gopalakrishnan, M. Knap, M. Müller, and E. Demler, Phys. Rev. Lett. 114, 160401 (2015).
- [20] P. Prelovšek, M. Mierzejewski, O. Barišić, and J. Herbrych, Ann. Phys. 529, 1600362 (2017).
- [21] F. Setiawan, D.-L. Deng, and J. H. Pixley, Phys. Rev. B 96, 104205 (2017).
- [22] R. Vasseur and J. E. Moore, J. Stat. Mech. Theory Exp 2016, 064010 (2016).
- [23] M. Žnidarič, A. Scardicchio, and V. K. Varma, Phys. Rev. Lett.
- 117, 040601 (2016). [24] H. S. Ruihua Fan, Pengfei Zhang and H. Zhai, Science Bul-
- letin **62**, 707 (2017). [25] X. Chen, T. Zhou, D. A. Huse, and E. Fradkin, Ann. Phys.
- **529**, 1600332 (2017). [26] Y. Huang, Y.-L. Zhang, and X. Chen, Ann. Phys. **529**,
- 1600318 (2017).
- [27] R.-Q. He and Z.-Y. Lu, Phys. Rev. B 95, 054201 (2017).
- [28] J. Li, R. Fan, H. Wang, B. Ye, B. Zeng, H. Zhai, X. Peng, and J. Du, Phys. Rev. X 7, 031011 (2017).
- [29] M. Gärttner, J. G. Bohnet, A. Safavi-Naini, M. L. Wall, J. J. Bollinger, and A. M. Rey, Nat. Phys. 13, 781 (2017).
- [30] E. V. H. Doggen, F. Schindler, K. S. Tikhonov, A. D. Mirlin, T. Neupert, D. G. Polyakov, and I. V. Gornyi, Phys. Rev. B 98, 174202 (2018).
- [31] A. Nico-Katz, A. Bayat, and S. Bose, Phys. Rev. Research 4, 033070 (2022).
- [32] T. Kohlert, S. Scherg, X. Li, H. P. Lüschen, S. Das Sarma, I. Bloch, and M. Aidelsburger, Phys. Rev. Lett. 122, 170403 (2019).
- [33] M. Schulz, C. A. Hooley, R. Moessner, and F. Pollmann, Phys. Rev. Lett. 122, 040606 (2019).
- [34] H. P. Lüschen, P. Bordia, S. Scherg, F. Alet, E. Altman, U. Schneider, and I. Bloch, Phys. Rev. Lett. 119, 260401 (2017).
- [35] P. Sierant and J. Zakrzewski, Phys. Rev. B 105, 224203 (2022).
- [36] T. Chanda and J. Zakrzewski, Phys. Rev. B 105, 054309 (2022).
- [37] A. Nico-Katz, A. Bayat, and S. Bose, Phys. Rev. B 105, 205133 (2022).
- [38] S. Sachdev, Quantum Phase Transitions (Cambridge University Press, 2011).
- [39] A. C. Potter, R. Vasseur, and S. A. Parameswaran, Phys. Rev. X 5, 031033 (2015).
- [40] P. Roushan, C. Neill, J. Tangpanitanon, V. M. Bastidas, A. Megrant, R. Barends, Y. Chen, Z. Chen, B. Chiaro, A. Dunsworth, et al., Science 358, 1175 (2017).
- [41] M. Rispoli, A. Lukin, R. Schittko, S. Kim, M. E. Tai, J. Léonard, and M. Greiner, Nature 573, 385 (2019).
- [42] M. Gong, G. D. de Moraes Neto, C. Zha, Y. Wu, H. Rong, Y. Ye, S. Li, Q. Zhu, S. Wang, Y. Zhao, et al., Phys. Rev. Research 3, 033043 (2021).

- [43] T. Chanda, P. Sierant, and J. Zakrzewski, Phys. Rev. Research 2, 32045 (2020).
- [44] I. Mondragon-Shem, A. Pal, T. L. Hughes, and C. R. Laumann, Phys. Rev. B 92, 064203 (2015).
- [45] Z. Xu, H. Huangfu, Y. Zhang, and S. Chen, New J. Phys. 22 (2020).
- [46] X. Wei, C. Cheng, G. Xianlong, and R. Mondaini, Phys. Rev. B 99, 165137 (2019).
- [47] B. Villalonga, X. Yu, D. J. Luitz, and B. K. Clark, Phys. Rev. B 97, 104406 (2018).
- [48] T. Devakul and R. R. P. Singh, Phys. Rev. Lett. 115, 187201 (2015).
- [49] A. Geißler and G. Pupillo, Phys. Rev. Research **2**, 042037 (2020).
- [50] W. De Roeck, F. Huveneers, M. Müller, and M. Schiulaz, Phys. Rev. B 93, 014203 (2016).
- [51] X. Wei, R. Mondaini, and G. Xianlong, arXiv:2001.04105.
- [52] Q. Guo, C. Cheng, Z.-H. Sun, Z. Song, H. Li, Z. Wang, W. Ren, H. Dong, D. Zheng, Y.-R. Zhang, et al., Nat. Phys. 17, 234 (2021).
- [53] C. Zha, V. M. Bastidas, M. Gong, Y. Wu, H. Rong, R. Yang, Y. Ye, S. Li, Q. Zhu, S. Wang, et al., Phys. Rev. Lett. 125, 170503 (2020).
- [54] K. Xu, J.-J. Chen, Y. Zeng, Y.-R. Zhang, C. Song, W. Liu, Q. Guo, P. Zhang, D. Xu, H. Deng, et al., Phys. Rev. Lett. 120 (2018).
- [55] B. Chiaro, C. Neill, A. Bohrdt, M. Filippone, F. Arute, K. Arya, R. Babbush, D. Bacon, J. Bardin, R. Barends, et al., arXiv:1910.06024.
- [56] Q. Guo, C. Cheng, H. Li, S. Xu, P. Zhang, Z. Wang, C. Song, W. Liu, W. Ren, H. Dong, et al., Phys. Rev. Lett. 127 (2021).
- [57] X. Mi, M. Ippoliti, C. Quintana, A. Greene, Z. Chen, J. Gross, F. Arute, K. Arya, J. Atalaya, R. Babbush, et al., Nature 601, 531 (2022).
- [58] M. Gong, H.-L. Huang, S. Wang, C. Guo, S. Li, Y. Wu, Q. Zhu, Y. Zhao, S. Guo, H. Qian, et al., arXiv:2201.05957.
- [59] M. Schreiber, S. S. Hodgman, P. Bordia, H. P. Lüschen, M. H. Fischer, R. Vosk, E. Altman, U. Schneider, and I. Bloch, Science 349, 842 (2015).
- [60] S. S. Kondov, W. R. McGehee, W. Xu, and B. DeMarco, Phys. Rev. Lett. 114, 083002 (2015).
- [61] P. Bordia, H. Lüschen, S. Scherg, S. Gopalakrishnan, M. Knap, U. Schneider, and I. Bloch, Phys. Rev. X 7, 041047 (2017).
- [62] P. Bordia, H. Lüschen, U. Schneider, M. Knap, and I. Bloch, Nat. Phys. 13, 460 (2017).
- [63] J.-y. Choi, S. Hild, J. Zeiher, P. Schauß, A. Rubio-Abadal, T. Yefsah, V. Khemani, D. A. Huse, I. Bloch, and C. Gross, Science 352, 1547 (2016).
- [64] A. Lukin, M. Rispoli, R. Schittko, M. E. Tai, A. M. Kaufman, S. Choi, V. Khemani, J. Léonard, and M. Greiner, Science 364, 256 (2019).
- [65] J. Smith, A. Lee, P. Richerme, B. Neyenhuis, P. W. Hess, P. Hauke, M. Heyl, D. A. Huse, and C. Monroe, Nat. Phys. 12, 907 (2016).
- [66] W. Morong, F. Liu, P. Becker, K. S. Collins, L. Feng, A. Kyprianidis, G. Pagano, T. You, A. V. Gorshkov, and C. Monroe, Nature 599, 393 (2021).
- [67] F. Rajabi, S. Motlakunta, C.-Y. Shih, N. Kotibhaskar, Q. Quraishi, A. Ajoy, and R. Islam, npj Quantum Inf. 5, 32 (2019)
- [68] S. Choi, J. Choi, R. Landig, G. Kucsko, H. Zhou, J. Isoya, F. Jelezko, S. Onoda, H. Sumiya, V. Khemani, et al., Nature 543, 221 (2017).

- [69] J. Choi, H. Zhou, S. Choi, R. Landig, W. W. Ho, J. Isoya, F. Jelezko, S. Onoda, H. Sumiya, D. A. Abanin, et al., Phys. Rev. Lett. 122, 043603 (2019).
- [70] T. Nguyen, N. Andrejevic, H. C. Po, Q. Song, Y. Tsurimaki, N. C. Drucker, A. Alatas, E. E. Alp, B. M. Leu, A. Cunsolo, et al., Nano Lett. 21, 7419 (2021).
- [71] R. K. Panda, A. Scardicchio, M. Schulz, S. R. Taylor, and M. Žnidarič, Epl 128 (2019).
- [72] A. Morningstar, L. Colmenarez, V. Khemani, D. J. Luitz, and D. A. Huse, Phys. Rev. B 105, 174205 (2022).
- [73] P. Sierant, M. Lewenstein, and J. Zakrzewski, Phys. Rev. Lett. 125, 156601 (2020).
- [74] F. Pietracaprina, N. Macé, D. J. Luitz, and F. Alet, SciPost Phys. 5, 45 (2018).
- [75] A. B. Harris, J. Phys. C: Solid State Phys. 7, 3082 (1974).
- [76] J. T. Chayes, L. Chayes, D. S. Fisher, and T. Spencer, Phys. Rev. Lett. 57, 2999 (1986).
- [77] A. Chandran, C. R. Laumann, and V. Oganesyan, arXiv:1509.04285.
- [78] J. Gray, S. Bose, and A. Bayat, Phys. Rev. B 97, 201105 (2018).
- [79] E. Levi, M. Heyl, I. Lesanovsky, and J. P. Garrahan, Phys. Rev. Lett. 116, 237203 (2016).
- [80] Z.-H. Sun, J. Cui, and H. Fan, Phys. Rev. Research 2, 013163 (2020)
- [81] P. T. Dumitrescu, A. Goremykina, S. A. Parameswaran, M. Serbyn, and R. Vasseur, Phys. Rev. B 99, 094205 (2019).
- [82] A. Goremykina, R. Vasseur, and M. Serbyn, Phys. Rev. Lett. 122, 040601 (2019).
- [83] A. Morningstar and D. A. Huse, Phys. Rev. B 99, 224205 (2019).
- [84] A. Morningstar, D. A. Huse, and J. Z. Imbrie, Phys. Rev. B 102, 125134 (2020).
- [85] J. Šuntajs, J. Bonča, T. c. v. Prosen, and L. Vidmar, Phys. Rev. E 102, 062144 (2020).
- [86] N. Laflorencie, G. Lemarié, and N. Macé, Phys. Rev. Research 2, 042033 (2020).
- [87] J. Šuntajs, J. Bonča, T. c. v. Prosen, and L. Vidmar, Phys. Rev. B 102, 064207 (2020).
- [88] M. Hopjan, G. Orso, and F. Heidrich-Meisner, Phys. Rev. B 104, 235112 (2021).
- [89] A. S. Aramthottil, T. Chanda, P. Sierant, and J. Zakrzewski, Phys. Rev. B 104, 214201 (2021).
- [90] S. Roy and D. E. Logan, SciPost Phys. 7 (2019).

- [91] R. M. Nandkishore and S. L. Sondhi, Phys. Rev. X 7, 041021 (2017).
- [92] N. Y. Yao, C. R. Laumann, S. Gopalakrishnan, M. Knap, M. Müller, E. A. Demler, and M. D. Lukin, Phys. Rev. Lett. 113, 243002 (2014).
- [93] R. Modak and T. Nag, Phys. Rev. E 101, 052108 (2020).
- [94] A. L. Burin, Phys. Rev. B 92, 104428 (2015).
- [95] S. Schiffer, J. Wang, X.-J. Liu, and H. Hu, Phys. Rev. A 100, 063619 (2019).
- [96] A. L. Burin, Phys. Rev. B 91, 094202 (2015).
- [97] K. S. Tikhonov and A. D. Mirlin, Phys. Rev. B 97, 214205 (2018).
- [98] A. O. Maksymov and A. L. Burin, Phys. Rev. B 101, 024201 (2020)
- [99] H. Li, J. Wang, X.-J. Liu, and H. Hu, Phys. Rev. A 94, 063625 (2016)
- [100] S. J. Thomson and M. Schiró, Phys. Rev. Research 2, 043368 (2020).
- [101] X. Deng, G. Masella, G. Pupillo, and L. Santos, Phys. Rev. Lett. 125, 010401 (2020).
- [102] M. Pino, Phys. Rev. B 90, 174204 (2014).
- [103] G. De Tomasi, Phys. Rev. B 99, 054204 (2019).
- [104] A. Safavi-Naini, M. L. Wall, O. L. Acevedo, A. M. Rey, and R. M. Nandkishore, Phys. Rev. A 99, 033610 (2019).
- [105] R. Singh, R. Moessner, and D. Roy, Phys. Rev. B 95, 094205 (2017).
- [106] S. Nag and A. Garg, Phys. Rev. B 99, 224203 (2019).
- [107] R. Modak and T. Nag, Phys. Rev. Research 2, 012074 (2020).
- [108] N. Roy and A. Sharma, Phys. Rev. B 97, 125116 (2018).
- [109] R. Yousefjani, S. Bose, and A. Bayat, arXiv:2201.03716.
- [110] D. N. Page, Phys. Rev. Lett. 71, 1291 (1993).
- [111] E. J. Torres-Herrera and L. F. Santos, Ann. Phys. 529, 1600284 (2017).
- [112] E. J. Torres-Herrera, J. Karp, M. Távora, and L. F. Santos, Entropy 18, 359 (2016).
- [113] J. Houdayer and A. K. Hartmann, Phys. Rev. B 70, 014418 (2004).
- [114] S. M. Bhattacharjee and F. Seno, J. Phys. A: Math. Gen. 34, 6375 (2001).
- [115] A. Sorge, pyfssa 0.7.6. Zenodo. (2015).
- [116] O. Melchert, arXiv:0910.5403.
- [117] T. C. Berkelbach and D. R. Reichman, Phys. Rev. B **81**, 224429 (2010).